Elastic Constants of Nematic Liquid Crystals

I. Theory of the Normal Deformation

HANS GRULER, TERRY J. SCHEFFER, and GERHARD MEIER

Institut für Angewandte Festkörperphysik der Fraunhofer-Gesellschaft, Freiburg i. Br.

(Z. Naturforsch. **27 a**, 966—976 [1972]; received 30 March 1972)

We present a theoretical treatment and give experimental observations of the deformation that occurs in a nematic liquid crystal when electric or magnetic fields are applied. We consider only normal deformations in the nematic material where fluid flow and other dynamic phenomena play no role. Three important sample geometries are considered in the magnetic field, and the experimentally observed deformations are in good agreement with theory. The normal deformation induced by electric fields is of interest from a device standpoint, and we give a solution for the deformation that is valid even for large dielectric anisotropies. This solution has been experimentally verified. We give a detailed comparison of the distortions produced by electric and magnetic fields and show that the deformations are of a similar form even though the field is nonuniform in the electric case. The change in birefringence and electrical capacitance as a function of distortion is discussed as a means of observing the deformation.

Many studies have been made on the electric and magnetic field induced deformations that occur in liquid crystals. ZOCHER was first to formulate the elastic deformations of liquid crystals in terms of a continuum theory, and he computed the normal deformation of a nematic liquid crystal in a magnetic field [1]. We use the term normal deformation here to describe the static distortions of a liquid crystal that do not involve fluid flow and other dynamic effects. In general this term applies equally well to the distortions produced by electric or magnetic fields. The actual form that the normal deformation takes is intimately related to the elastic constants of the liquid crystal, and this relationship offers one important means of evaluating these elastic constants. SAUPE has computed the form of the magnetic field induced deformations in nematics for the case of unequal elastic constants which enabled him to evaluate the bend and splay elastic constants for p-azoxyanisole (PAA) [2]. There has been much recent experimental activity dealing with electric field induced normal deformations in nematics [3, 4], but only the beginnings of a general theory have heretofore been given [5].

In this paper we give a complete theory for the electric field induced normal deformation in nematics and present additional information describing the normal deformation produced by magnetic fields.

Reprint requests to H. GRULER, Institut für Angewandte Festkörperphysik, *D-7800 Freiburg i. Br.*, Eckerstraße 4.

We will show how the elastic constants can be evaluated from the various deformations.

I. The Normal Deformation

The form of the distortions in a nematic liquid crystals induced by magnetic or electric fields is determined by the elastic constants. For simple geometries having known boundary conditions, the exact form of the distortion can be calculated, and the elastic constants can be evaluated from the actual measurements of the field induced deformation.

Consider the case of a nematic liquid crystal confined between two parallel glass plates that have been specially treated so that the orientation of the optical axis at the boundary is uniform and rigidly fixed. For planar structures the distortional energy in a volume, V, can be written [6]

$$G_{\text{elastic}} = \tfrac{1}{2}\int_V \{k_{11}(\operatorname{div}\boldsymbol{L})^2 + k_{22}(\boldsymbol{L}\cdot\operatorname{curl}\boldsymbol{L})^2 + k_{33}(\boldsymbol{L}\times\operatorname{curl}\boldsymbol{L})^2\}\,\mathrm{d}\tau\,. \quad (1)$$

ZOCHER [1] named the elastic constants k_{ii} as splay (Auffächerung oder Querbiegung), twist, and bend (Längsbiegung) for $i = 1, 2$ and 3 respectively (see Fig. 1). $\boldsymbol{L}$ is a unit vector parallel to the local optical axis and is defined at each point in the liquid crystal.

A. Magnetic Fields

One way to compute the deformation of the nematic liquid crystal in a magnetic field is to con-

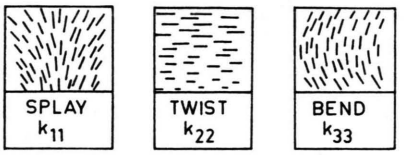

Fig. 1. Schematic illustration of various pure elastic deformations in nematic liquid crystals and their associated elastic constants. The lines indicate the orientation of the director or local optical axis at various points in space. Only the projection of the director in the plane of the figure is given for the twist case.

sider the sample as part of a larger closed system where the total energy is conserved. In making a virtual deformation in the liquid crystal (i. e. changing the orientation of $\boldsymbol{L}$ in some part of the sample) conservation of energy requires that:

$$\mathrm{d}G_{\text{elastic}} + \mathrm{d}G_{\text{magnetic}} = \mathrm{d}G_{\text{source}} . \tag{2}$$

$\mathrm{d}G_{\text{elastic}}$ and $\mathrm{d}G_{\text{magnetic}}$ are the changes in the total elastic and magnetic energies stored in the liquid crystal respectively, and $\mathrm{d}G_{\text{source}}$ is the necessary work performed by external energy sources to bring about these changes. It can be shown that for a current-stabilized electromagnet **

$$\mathrm{d}G_{\text{source}} = 2\,\mathrm{d}G_{\text{magnetic}} .$$

$\mathrm{d}G_{\text{source}}$ can be eliminated from Eq. (2), giving

$$\mathrm{d}G_{\text{elastic}} - \mathrm{d}G_{\text{magnetic}} = 0 .$$

This is equivalent to requiring that in the equilibrium configuration

$$G_{\text{elastic}} - G_{\text{magnetic}} \tag{3}$$

have an extreme value with respect to variations of $\boldsymbol{L}$. The total energy of the sample, $G_{\text{elastic}} + G_{\text{magnetic}}$, is not minimized, as one might think at first.

The total magnetic energy in the sample is

$$G_{\text{magnetic}} = \tfrac{1}{2} \int_V \boldsymbol{B}\cdot\boldsymbol{H}\,\mathrm{d}\tau$$

where $\boldsymbol{B}$ is the magnetic induction and $\boldsymbol{H}$ is the magnetic field. In general $\boldsymbol{B}$ and $\boldsymbol{H}$ are not parallel for anisotropic materials, but in nematic liquid crystals the diamagnetic susceptibilities are so small that the angle between $\boldsymbol{B}$ and $\boldsymbol{H}$ is negligible. For small susceptibilities

$$G_{\text{magnetic}} = \tfrac{1}{2} \int_V \{(1+\chi_1)\,(\boldsymbol{L}\cdot\boldsymbol{H})^2 + (1+\chi_2)\,(\boldsymbol{L}\times\boldsymbol{H})^2\}\,\mathrm{d}\tau \tag{4}$$

** See for example: Foundations of Electromagnetic Theory, by J. R. Reitz and F. J. Milford, Addison-Wesley Co. Inc., Reading, Mass., 1962, p. 234.

where χ_1 and χ_2 are the components of the magnetic susceptibility parallel and perpendicular to the local optical axis. The diamagnetic susceptibility anisotropy $\Delta\chi = \chi_1 - \chi_2$ has a positive sign for nematic liquid crystals containing aromatic rings. Non-aromatic nematics, however, such as compensated cholesteric mixtures, can have a negative $\Delta\chi$ [7].

Equations (1) and (4) are substituted into (3) and the method of calculus of variation is applied to give a second order differential equation, the solution of which describes the orientation of $\boldsymbol{L}$ throughout the sample. The resulting deformation will be discussed for several boundary conditions and geometries in the following 3 cases. These particular cases are important for experimentally determining the elastic constants k_{11}, k_{22} and k_{33}.

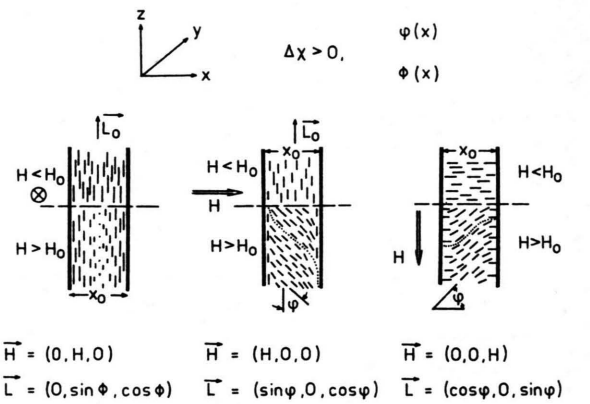

Fig. 2. Illustration of the geometries and the normal deformations above and below threshold for the cases discussed in the text. Cases 1, 2, and 3 are shown from left to right.

1. Case 1

For the special case where the undisturbed optical axis $\boldsymbol{L}_0$ is parallel to the two glass plates and $\boldsymbol{H}$ is perpendicular to $\boldsymbol{L}_0$ and parallel to the glass plates (Fig. 2), only the twist elastic constant k_{22} comes into play. We can describe the resulting deformation by a single parameter Φ, the angle between the local optical axis defined at each point in the sample and $\boldsymbol{L}_0$.

The Euler-Lagrange equation resulting from the requirement that (3) have an extreme value is

$$k_{22}\frac{\mathrm{d}^2\Phi}{\mathrm{d}x^2} + \Delta\chi\,H^2 \sin\Phi\cos\Phi = 0 . \tag{5 a}$$

This can be written

$$\frac{\mathrm{d}}{\mathrm{d}x}\left[\left(\frac{\mathrm{d}\Phi}{\mathrm{d}x}\right)^2 + \frac{\Delta\chi\,H^2}{k_{22}}\sin^2\Phi\right] = 0 , \tag{5 b}$$

which is solved to give

$$\frac{H}{H_0} = \frac{2}{\pi}\int_0^{\Phi_M} (\sin^2 \Phi_M - \sin^2 \Phi)^{-1/2}\, d\Phi$$
$$= 1 + \tfrac{1}{4}\,\Phi_M^2 + \tfrac{11}{196}\,\Phi_M^4 + \ldots \qquad (6)$$

$$\frac{x}{x_0} = \frac{H_0}{\pi H}\int_0^{\Phi} (\sin^2 \Phi_M - \sin^2 \Phi)^{-1/2}\, d\Phi = \frac{1}{\pi}\arcsin\frac{\Phi}{\Phi_M}$$
$$- \Phi(\Phi_M^2 - \Phi^2)^{1/2}\,\frac{(1 + \tfrac{11}{16}\,\Phi_M^2 + \tfrac{1}{8}\,\Phi^2 + \ldots)}{12\,\pi(1 + \tfrac{1}{4}\,\Phi_M^2 + \tfrac{11}{196}\,\Phi_M^4 + \ldots)} \qquad (7)$$

where

$$H_0 = \frac{\pi}{x_0}\,(k_{22}/\Delta\chi)^{1/2}. \qquad (8)$$

Φ_M is the maximum deformation angle which for reasons of symmetry is assumed to occur in the center of the film and x_0 is the film thickness. Equation (6) shows that there is a threshold field, H_0, below which no deformation can occur [8]. The integrals in (6) and (7) are elliptic of the first kind. Both Eqs. (6) and (7) must be used to compute the deformation at an arbitrary point in the liquid crystal. Equation (6) gives the relationship between Φ_M in the center of the sample and the applied field, and Eq. (7) relates the deformation angle throughout the film to Φ_M. We have indicated the small angle approximations to these equations which are valid near the threshold field. From symmetry (6) can contain only terms of even power in Φ_M.

This deformation is difficult to observe optically because the plane of polarizaton of a normally incident light beam is rotated on either side of the sample midplane by exactly equal and opposite amounts when the pitch of the twist is longer than the wavelength of the light used in observation. With obliquely incident light, however, it is possible to observe the deformation because Snell's law predicts total reflection even for small deformations if the angle of incidence is large enough. FRÉEDERICKSZ et al. used this technique to determine k_{22} for p-azoxyanisole from the threshold condition given by Equation (8) [9].

2. Case 2

The geometry in this case is similar to case 1, except that the magnetic field has been rotated 90° making it perpendicular to the glass plates (Fig. 2). As in case 1, the deformation throughout the sample can be described by a parameter φ which is the angle between the local optical axis $\boldsymbol{L}$ and $\boldsymbol{L}_0$, where $\boldsymbol{L}$ is always in the plane defined by $\boldsymbol{H}$ and $\boldsymbol{L}_0$. The variational problem for arbitrary k_{ii} has been solved by SAUPE [2]. The resulting Euler-Lagrange equation is

$$\frac{d}{dx}\left[(k_{11}\cos^2\varphi + k_{33}\sin^2\varphi)\left(\frac{d\varphi}{dx}\right)^2 + \Delta\chi\, H^2 \sin^2\varphi\right] = 0. \qquad (9)$$

This equation is solved to give

$$\frac{H}{H_0} = \frac{2}{\pi}\int_0^{\varphi_M}\left\{\frac{1 + \varkappa\sin^2\varphi}{\sin^2\varphi_M - \sin^2\varphi}\right\}^{1/2} d\varphi$$
$$= 1 + \tfrac{1}{4}\,(\varkappa+1)\,\varphi_M^2 + \ldots, \qquad (10)$$

$$\frac{x}{x_0} = \frac{H_0}{\pi H}\int_0^{\varphi}\left\{\frac{1 + \varkappa\sin^2\varphi}{\sin^2\varphi_M - \sin^2\varphi}\right\}^{1/2} d\varphi$$
$$= \frac{1}{\pi}\arcsin\frac{\varphi}{\varphi_M} - \varphi(\varphi_M^2 - \varphi^2)^{1/2} \qquad (11)$$
$$\cdot\,\frac{1 + 3\varkappa + \ldots}{12\,\pi(1 + \tfrac{1}{4}\,(\varkappa+1)\,\varphi_M^2 + \ldots)},$$

$$H_0 = \frac{\pi}{x_0}\,(k_{11}/\Delta\chi)^{1/2}, \qquad (12\,a)$$

$$\varkappa = (k_{33} - k_{11})/k_{11}.$$

As before, φ_M is the maximum deformation angle occurring in the center of the sample. As is clear from Eq. (9), the deformation depends on both the splay and bend elastic constants k_{11} and k_{33}; the twist constant k_{22} does not enter into the problem. Note that the threshold field, however, depends only on the splay elastic constant k_{11}. The solution takes the same general form as in case 1, except that now the integrals are elliptic of the third kind.

Unlike case 1, however, this deformation is easily observed with normaly incident polarized light and offers a good method to measure k_{11} and k_{33}.

3. Case 3

A third important geometry is the perpendicularly oriented or homeotropic film geometry. Here $\boldsymbol{L}_0$ is perpendicular to the glass plates and $\boldsymbol{H}$ is perpendicular to $\boldsymbol{L}_0$ (Fig. 2). Equations (9) – (12) are also valid for this case except that the elastic con-

stants k_{11} and k_{33} must be interchanged. In this case the threshold field depends only on the bend elastic constant k_{33}

$$H_0 = \frac{\pi}{x_0} (k_{33}/\Delta\chi)^{1/2}. \qquad (12\,b)$$

The deformations occurring in case 2 and 3 are summarized in Figure 3.

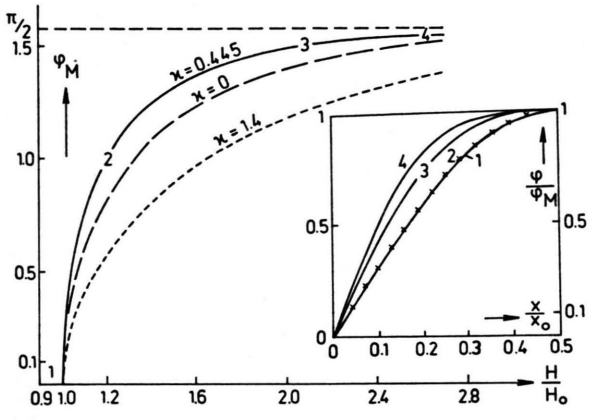

Fig. 3. The calculated maximum deformation angle φ_M vs. reduced field H/H_0 for various elastic constant anisotropies $\varkappa$ in parallel oriented and homeotropic samples. The curves in the inset show the reduced deformation in terms of φ_M for the case $\varkappa = -0.445$ at the 4 different fields indicated by 1–4. Note that in this reduced representation there is no significant difference in the deformation between the field at 1 (solid line) and the field at 2 (crosses). (The upper curve should read $\varkappa = -0.445$.)

4. Observation with Polarized Light

A simple but effective method to experimentally measure the deformations occurring in cases 2 and 3 makes use of the birefringence of the nematic liquid crystal. Nematic liquid crystals are uniaxial and therefore a normally incident polarized monochromatic light beam splits inside the crystal into an ordinary beam and extraordinary beam. The electric field vector of the ordinary beam is always perpendicular to the optical axis, and therefore propagates with a velocity determined by the ordinary refractive index n_0. The extraordinary ray is polarized 90° to this direction and its average velocity is determined by an effective refractive index given by

$$n_{\text{eff}} = \frac{1}{x_0} \int_0^{x_0} n(\varphi)\, dx, \qquad (13)$$

where for the parallel oriented sample (case 2)

$$n(\varphi) = n_e n_0 (n_e^2 \sin^2\varphi + n_0^2 \cos^2\varphi)^{-1/2}. \qquad (14)$$

n_e is the extraordinary index of refraction. It is clear rom Eqs. (13) and (14) that n_{eff} depends on the deformation angle φ throughout the sample. The phase difference d existing between the two beams on the other side of the sample is given by

$$d(H) = \frac{x_0}{\lambda} (n_{\text{eff}} - n_0). \qquad (15)$$

The maximum value of $d(H)$ occurs at $H = 0$. SAUPE [2] defined a phase difference decrease, δ, by

$$\delta = |d(0) - d(H)|. \qquad (16)$$

For case 2 δ can be related to the reduced field H/H_0 by

$$\delta = \frac{x_0 n_e}{\lambda} \left| 1 - \frac{2H}{\pi H_0} \int_0^{\varphi_M} \frac{(1+\varkappa \sin^2\varphi)^{1/2}\, d\varphi}{(1+\nu \sin^2\varphi)^{1/2} (\sin^2\varphi_M - \sin^2\varphi)^{1/2}} \right|, \qquad (17\,a)$$

$$\delta = \frac{x_0 n_e}{\lambda} \nu \left| \frac{H - H_0}{H_0} \frac{1}{\varkappa+1} - \left(\frac{H-H_0}{H_0}\right)^2 \left(\frac{1}{\varkappa+1}\right)^2 \left(3 + \tfrac{9}{4}\nu - \tfrac{5}{4}(\varkappa+1)\right) + \ldots \right|, \qquad (17\,b)$$

$$\nu = (n_e^2 - n_0^2)/n_0^2.$$

Equations (17) apply equally well to the homeotropic case 3 if n_e and n_0 as well as k_{11} and k_{33} are interchanged in all the equations. It is clear that measurements of δ at various fields can give k_{11} and k_{33}.

This phase difference can be easily measured by placing the sample between crossed polarizers and illuminating it with monochromatic light. The experimental apparatus is illustrated in Figure 4. A parallel monochromatic light beam is normally incident to the sample located between crossed polarizers in the magnet gap. The transmitted light is detected at a selected point on the sample with a photomultiplier. The y-axis of the recorder is proportional to this transmitted intensity, and the x-axis is driven by a Hall effect device making it proportional to

the field. Changes in the phase difference as the field is varied appear as an oscillating curve. Typical curves are illustrated in Fig. 5 for hexyloxyazoxybenzene at various temperatures. The sudden appearance of the oscillations occurs at the threshold field. In Fig. 6 a comparison is given between the experimental phase difference decrease δ for PAA as a function of magnetic field and the phase difference calculated from Eqs. (10) and (17 a). The data points correspond to the maxima and minima of the oscillating curves similar to those given in Figure 5. We fitted the curve to the data using a two parameter non-linear least squares fitting program for implicit functions developed by DEULING [10]. One parameter is the threshold field H_0 which gives k_{11}, and the other parameter is the ratio k_{33}/k_{11}.

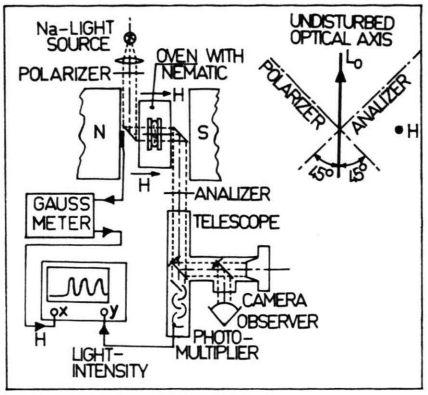

Fig. 4. The experimental arrangement used to detect the normal deformation in the parallel oriented geometry.

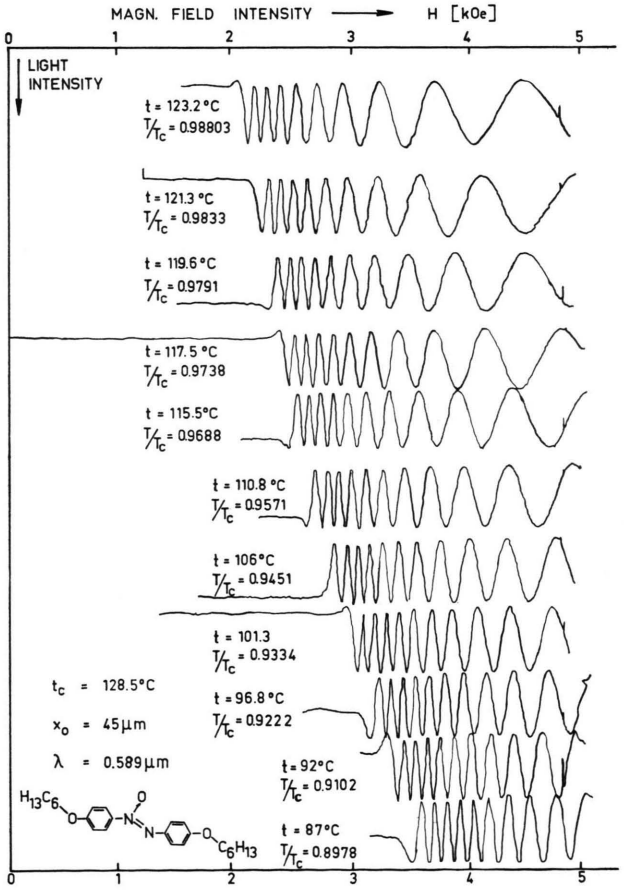

Fig. 5. The interference oscillations caused by a continuous change in sample birefringence are illustrated in this raw recorder trace for hexyloxyazoxybenzene at various temperatures. The sudden onset of oscillations indicates the threshold field. (Only measurements up to 5 kOe are given.)

The agreement with theory is excellent, even in relatively high fields. In still higher fields ($H/H_0 \geqq 4$), however, the agreement is only fair. SNYDER and SAUPE [11] believe this discrepancy is due to inaccuracies in the measured refractive index values, because the curve is very sensitive to small changes in the birefringence $\Delta n = n_e - n_0$. Snyder and Saupe used a wedge-shaped sample cell as described in Ref. [2] and therefore measure Δn in the same specimen used for the deformation measurements. They found good agreement of the phase difference decrease δ with theory up to very high fields ($H/H_0 = 10$). We measured Δn in a separate variable thickness cell, however, and this introduces more uncertainty. Assuming the theory is valid at high fields, Δn can also be determined by an iterative procedure described in Section II A.

Near the threshold field a slight rounding off of the δ vs. field curve occurs as shown in the inset of Figure 6. This rounding off is not predicted by Eqs. (10) and (17 a) but thermal energy, kT, could to be responsible for this effect. The highly correlated but thermally disoriented regions that produce the characteristic sparkling effect often seen in nematics have a very weak restoring force near threshold for those regions where the instantaneous optical axis $\boldsymbol{L}$ is in a plane defined by $\boldsymbol{L}_0$ and $\boldsymbol{H}$. Therefore, on the average, n_{eff} is less than n_e even before the threshold field is achieved. This rounding off might also be explained by a deviation of the magnetic field from a direction normal to the undisturbed optical axis. DAFERMOS [8] and RAPINI and PAPOULAR [14] showed that a true threshold field can never exist for this case.

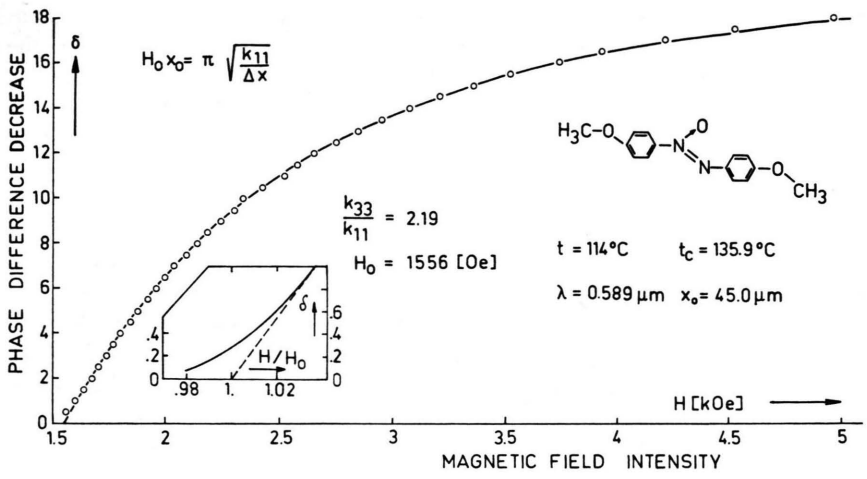

Fig. 6. Comparison between experimental values and the least squares fitted theoretical curve for the phase difference decrease δ vs. magnetic field in a parallel oriented p-azoxyanisole sample. The inset shows the slight rounding off observed near the threshold field believed to be caused by thermal fluctuations.

The agreement between theory and experiment is also good for the homeotropic oriented sample in case 3. Reasonable care must be taken, however, to insure a well defined perpendicular orientation at the glass boundaries. In many cases this can be accomplished by adding special dopants [12, 13] or treating the glass surfaces in special ways [4]. SAUPE [2], for example, obtained a well oriented PAA film by cleaning the glass surfaces with a hot sodium dichromate-sulfuric acid cleaning solution. A poorly defined boundary orientation will give threshold values $H_0 x_0$ that depend on the sample thickness x_0 (l. c. [14]).

B. Electric Fields

1. Mathematical Treatment

Electric fields can interact with the anisotropic dielectric susceptibility of nematic liquid crystals to produce qualitatively the same deformation that is observed in magnetic fields. There is one important difference. In the magnetic case the susceptibilities are small enough so that the magnetic field vector $\boldsymbol{H}$ and magnetic induction vector $\boldsymbol{B}$ are essentially parallel. The analogy for electric fields breaks down because the dielectric susceptibilities of nematics are large and the electric field vector $\boldsymbol{E}$ can no longer be considered parallel to the electric displacement vector $\boldsymbol{D}$. This results in a nonuniform electric field in the sample [5].

The electric energy in a volume V, G_{electric}, is given by the general relation

$$G_{\text{electric}} = \tfrac{1}{2} \int_V \boldsymbol{D} \cdot \boldsymbol{E} \, d\tau \,. \tag{18}$$

Consider an arbitrary deformation in the sample $\varphi(x)$ of the type described in the magnetic case 2. The condition

$$\operatorname{curl} \boldsymbol{E} = 0 \tag{19}$$

requires that $E_y = E_z = 0$ because $\varphi(x)$ is a deformation depending only on the x-direction. If the effects of space charges can be neglected the additional condition

$$\operatorname{div} \boldsymbol{D} = 0 \tag{20}$$

gives the following relationship between the electric field and the deformation:

$$E_x(x) = \frac{U}{(1 + (\Delta\varepsilon/\varepsilon_2) \sin^2\varphi) \int_{\langle x_0 \rangle} (1 + (\Delta\varepsilon/\varepsilon_2) \sin^2\varphi)^{-1} \, dx} \,, \tag{21}$$

$$\Delta\varepsilon = \varepsilon_1 - \varepsilon_2 \,,$$

ε_1 and ε_2 are the dielectric constants measured parallel and perpendicular to the optical axis respectively, and U is the electric potential applied to the electrodes. The electric field clearly depends on the location in the film ***. From (20) and (21) we obtain

$$D_x = U \, \varepsilon_2 \, \varepsilon_0 / \int_{\langle x_0 \rangle} (1 + (\Delta\varepsilon/\varepsilon_2) \sin^2\varphi)^{-1} \, dx \,. \tag{22}$$

D_x is uniform throughout the sample. Substituting (22) and (21) into (18) we obtain

$$G_{\text{electric}} = \tfrac{1}{2} U^2 \varepsilon_2 \varepsilon_0 \frac{1}{\int_{\langle x_0 \rangle} (1 + \Delta\varepsilon/\varepsilon_2) \sin^2\varphi)^{-1} \, dx} = \frac{1}{2} \frac{D_x^2}{\varepsilon_0 \varepsilon_2} \int_{\langle x_0 \rangle} \frac{dx}{1 + (\Delta\varepsilon/\varepsilon_2) \sin^2\varphi} \,. \tag{23}$$

*** In the case that the electric field is applied parallel to the glass plates, however, a deformation can occur as in case 2 or 3 but the field will be completely uniform in the sample.

This expresses the total electric energy per unit area in terms of the deformation $\varphi(x)$. To proceed further, it is necessary to consider the sample as part of a system where the total energy is conserved. This means that

$$dG_{\text{elastic}} + dG_{\text{electric}} = dG_{\text{source}} .$$

As in the magnetic case, dG_{source} is the work performed by external energy sources. In the electric field case, however, there are two possible ways to make the virtual deformation; it can be made either under conditions of constant potential or constant charge. For the constant potential case

$$dG_{\text{source}} = 2\, dG_{\text{electric}} ,$$

and the variational problem requires that

$$G_{\text{elastic}} - G_{\text{electric}}$$

have an extreme value. The resulting Euler-Lagrange differential equation for the parallel oriented sample is then [15]

$$\frac{d}{dx}\left[\left(\frac{d\varphi}{dx}\right)^2 (k_{11}\cos^2\varphi + k_{33}\sin^2\varphi) - \frac{D_x^2}{\varepsilon_0\,\varepsilon_2}\left(1+\frac{\Delta\varepsilon}{\varepsilon_2}\sin^2\varphi\right)^{-1}\right] = 0 . \quad (24)$$

There are no external energy sources in the constant charge case and therefore $dG_{\text{source}} = 0$. Now the variational problem requires an extreme value for

$$G_{\text{elastic}} + G_{\text{electric}} .$$

In this case the total energy of the system does have a minimum value. It is worthwhile to note that for constant charge, D_x is independent of the deformation in the sample, as well as being independent of position. The resulting Euler-Lagrange differential equation is identical to (24). This equality could have been foreseen because the deformation in the liquid crystal can only depend on the final potential difference between the electrodes and not on the method used to obtain this potential.

At this point one should mention that if the air gap of the current-stabilized electromagnet is filled with the nematic liquid crystal then the magnetic tension $U_m = \int_0^{x_0} H(\varphi)\, dx$ is a constant independent of deformation. In general, the magnetic case corresponds to the electric case under conditions of constant potential.

Equation (24) can be solved in a manner similar to the magnetic case giving

$$\frac{U}{U_0} = \frac{2}{\pi}\left(1+\frac{\Delta\varepsilon}{\varepsilon_2}\sin^2\varphi_M\right)^{1/2}\int_0^{\varphi_M}\left\{\frac{1+\varkappa\sin^2\varphi}{(1+(\Delta\varepsilon/\varepsilon_2)\sin^2\varphi)(\sin^2\varphi_M-\sin^2\varphi)}\right\}^{1/2} d\varphi , \quad (25\,a)$$

$$U/U_0 = 1 + \tfrac{1}{4}\left(\varkappa + (\Delta\varepsilon/\varepsilon_2) + 1\right)\varphi_M^2 + o\,(\varphi_M^4), \quad (25\,b)$$

$$\frac{x}{x_0} = \int_0^{\varphi}\left\{\frac{(1+\varkappa\sin^2\varphi)\,(1+(\Delta\varepsilon/\varepsilon_2)\sin^2\varphi)}{\sin^2\varphi_M-\sin^2\varphi}\right\}^{1/2} d\varphi \Big/ \int_0^{\varphi_M}\left\{\frac{(1+\varkappa\sin^2\varphi)\,(1+(\Delta\varepsilon/\varepsilon_2)\sin^2\varphi)}{\sin^2\varphi_M-\sin^2\varphi}\right\}^{1/2} d\varphi , \quad (26\,a)$$

$$\frac{x}{x_0} = \frac{1}{\pi}\arcsin\frac{\varphi}{\varphi_M} - \varphi(\varphi_M^2-\varphi^2)^{1/2}\,\frac{1+3\left(\varkappa+(\Delta\varepsilon/\varepsilon_2)\right)+\ldots}{12\,\pi[1+\tfrac{1}{4}\left(\varkappa+(\Delta\varepsilon/\varepsilon_2)+1\right)\varphi_M^2+\ldots]} , \quad (26\,b)$$

$$U_0 = \pi(k_{11}/\varepsilon_0\,\Delta\varepsilon)^{1/2} . \quad (27)$$

U is the applied potential difference under conditions of constant potential, and is the final potential difference under conditions of constant charge. Equation (25 b) shows that there is a threshold field which is completely analogous to the magnetic case. Unlike the magnetic case, however, the form of the deformation above threshold depends on the additional parameter $\Delta\varepsilon/\varepsilon_2$. It is clear from the small angle approximations (10), (11) and (25 b), (26 b) that the form of the normal deformation near threshold is similar in both magnetic and electric fields. The above derivation applies equally well to the homeotropic case if k_{11} is interchanged with k_{33} and ε_1 is interchanged with ε_2.

2. Observation with Polarized Light

As was described earlier for magnetic fields, the extent of the deformation can be measured from the

change in birefringence observed in the sample. The phase difference decrease δ as a function of the maximum angle φ_M in the center of the parallal oriented sample is

$$\delta = \frac{x_0}{\lambda} n_e \left\{ 1 - \int_0^{\varphi_M} \left\{ \frac{(1+\varkappa \sin^2\varphi)\,(1+(\Delta\varepsilon/\varepsilon_2)\sin^2\varphi)}{(1+\nu\sin^2\varphi)\,(\sin^2\varphi_M - \sin^2\varphi)} \right\}^{1/2} d\varphi \Big/ \int_0^{\varphi_M} \left\{ \frac{(1+\varkappa\sin^2\varphi)\,(1+(\Delta\varepsilon/\varepsilon_2)\sin^2\varphi)}{\sin^2\varphi_M - \sin^2\varphi} \right\}^{1/2} d\varphi \right\}, \tag{28 a}$$

$$\delta = \frac{x_0}{\lambda} n_e \nu \frac{U-U_0}{U_0} \frac{1}{\varkappa + 1 + (\Delta\varepsilon/\varepsilon_2)} + o\left(\frac{U-U_0}{U_0}\right)^2. \tag{28 b}$$

The field dependence of δ enters in through the field dependence of φ_M which is given in Equation (25). The expression for small angles shows the same linear relationship between δ and the reduced field U/U_0 as was observed in the magnetic case. For larger reduced fields the functional form is of course different. A comparison of the electric and magnetic field results is given in Fig. 7 for a mixture of 82.09% p-methoxybenzylidene-p-butylaniline (MBBA) and 7.91% p-(p-butoxybenzylidene)-aminobenzonitrile. To minimize error, the identical sample was used in both the electric and magnetic field experiments, and the phase difference decrease was measured at exactly the same point in the sample. The mixture was confined between two parallel, semitransparent, SnO_2-coated glass plates spaced 27.0 μ apart. The magnetic field was applied perpendicular to the plates, or alternatively, an electric potential difference was applied to the two conducting SnO_2 surfaces.

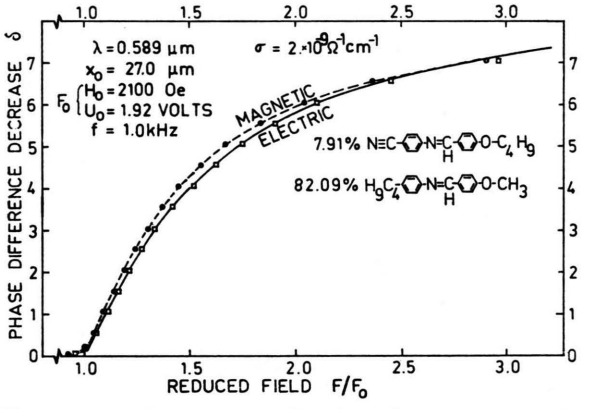

Fig. 7. Comparison between electric and magnetic field induced deformations of a mixed nematic on a reduced field scale.

The dashed curve in Fig. 7 fits the experimental points and was computed from Eqs. (10) and (17) assuming $k_{33}/k_{11} = 1.7$ and $H_0 = 2100$ Oersteds. These parameters are then used in Eqs. (25 a) and (28 a) and only $\Delta\varepsilon/\varepsilon_2$ is varied to fit the electric field data. The unbroken curve in Fig. 7 was computed assuming $\Delta\varepsilon/\varepsilon_2 = 0.30$. The actual dielectric constants of the mixture have not yet been measured, but a value of $\Delta\varepsilon/\varepsilon_2 = 0.23$ can be estimated from the dielectric values of similar nematic benzonitriles [16] and of MBBA [17]. The good agreement with theory supports the validity of our assumption that the effects of space charge can be ignored [Eq. (20)] and that hydrodynamic flow and electrical conduction play no role in the deformation.

3. Measuring Deformation by Capacitance Change

The change in capacitance can also be used to measure the extent of the deformation occurring in the liquid crystal [18, 19]. The capacitance C per unit area can be computed from Eq. (23) using

$$C = 2\,G_{\text{electric}}/U^2.$$

If an electric field is used to produce the deformation, then Eqs. (23) and (24) give

$$C_{\text{electric}} = \frac{\varepsilon_0\,\varepsilon_2}{x_0} \int_0^{\varphi_M} \left\{ \frac{(1+\varkappa\sin^2\varphi)\,(1+(\Delta\varepsilon/\varepsilon_2)\sin^2\varphi)}{\sin^2\varphi_M - \sin^2\varphi} \right\}^{1/2} d\varphi \Big/ \int_0^{\varphi_M} \left\{ \frac{1+\varkappa\sin^2\varphi}{(1+(\Delta\varepsilon/\varepsilon_2)\sin^2\varphi)\,(\sin^2\varphi_M - \sin^2\varphi)} \right\}^{1/2} d\varphi \tag{29 a}$$

and

$$C_{\text{electric}} = \frac{\varepsilon_0\,\varepsilon_2}{x_0} \left\{ 1 + \frac{U-U_0}{U_0} \frac{2(\Delta\varepsilon/\varepsilon_2)}{\varkappa + (\Delta\varepsilon/\varepsilon_2) + 1} + o\left(\frac{U-U_0}{U_0}\right)^2 \right\}. \tag{29 b}$$

Of course the field used to measure the capacitance must be much smaller than the field used to produce the deformation. A slightly different form for the capacitance is obtained from Eqs. (9) and (10) when the deformation is induced by a magnetic field.

$$C_{\text{magnetic}} = \frac{\varepsilon_0 \varepsilon_2}{x_0} \frac{\pi}{2} \frac{H}{H_0} \frac{1}{\int_0^{\varphi_M} \left\{ \frac{1 + \varkappa \sin^2 \varphi}{(1 + (\Delta\varepsilon/\varepsilon_2) \sin^2 \varphi)^2 (\sin^2 \varphi_M - \sin^2 \varphi)} \right\}^{1/2} d\varphi}, \tag{30 a}$$

$$C_{\text{magnetic}} = \frac{\varepsilon_0 \varepsilon_2}{x_0} \left\{ 1 + \frac{H - H_0}{H_0} \frac{2(\Delta\varepsilon/\varepsilon_2)}{\varkappa + 1} + o\left(\left(\frac{H - H_0}{H_0} \right)^2 \right) \right\}. \tag{30 b}$$

This capacitance method, however, suffers from a serious disadvantage. In order to obtain meaningful results, the entire sample must be perfectly oriented. This state is rarely achieved in typical samples, because there are usually regions where the orientation is not uniform due to poor surface alignment, edge effects, etc. These nonuniform regions have no threshold field and therefore they will produce a long tail on the capacitance vs. field curve that would otherwise be expected to show a sharp threshold. This rounding off makes analysis extremely difficult. With the optical birefringence method, on the other hand, particularly well oriented portions of the sample can be selected for measurement and the nonuniform regions can be ignored. The sampling area is about 1 mm² for the measurements shown in Figures 6 and 7.

II. Application to Elastic Constant Measurement

A. k_{11}, k_{22}, and k_{33} Obtained from the Normal Deformation of Parallel and Homeotropic Samples

In Section I we have shown that measurements of the normal deformation can give values of the elastic constants in terms of the susceptibility anisotropy. Separate measurements of the susceptibilities are required to obtain the actual values of the elastic constants [20–22]. In the following discussion it will be assumed that all susceptibilities are known.

It is possible to determine the three elastic constants k_{11}, k_{22}, and k_{33} separately and independently by measuring only the threshold fields of the specimen in the appropriate geometries [see Fig. 2 and Eqs. (8), (12 a) and (12 b)]. This was the method used by FRÉEDERICKSZ et al. [23, 24] and other early workers. This method is simple and does not require refractive index measurements, but it does require at least two different samples.

SAUPE [2] showed that the form of the normal deformation above threshold depends upon the elastic constant ratio k_{33}/k_{11}. For a parallel oriented sample (Case 2), k_{11} is obtained from the threshold, and k_{33} can then be determined from the deformation above threshold. Case 1 is obtained by rotating the same sample 90° in the magnetic field, and then k_{22} can be determined using Fréedericksz's total reflection method [9]. Refractive index data is required, however, to obtain k_{33}. The intrinsic birefringence of the liquid crystal Δn, is almost equal to the change in refractive index of a parallel oriented sample, $n_e - n_{\text{eff}}$, when a large field is applied to make the optical axis nearly perpendicular to the glass plates. $\lim_{H \to \infty} (n_e - n_{\text{eff}}) = \Delta n$. The maximum phase difference decrease $\delta_{\max}$ is easily estimated by extrapolating an experimental curve such as is given in Fig. 6 to high fields, and Δn can be estimated from $\Delta n = \delta_{\max} \lambda / x_0$.

Assuming that the normal deformation theory is correct even at relatively high reduced fields [11], Δn can be precisely determined by an iterative procedure because the high field region of the phase difference curve is very sensitive to small changes in Δn. Values of n_0 are also needed and these can be determined in an ordinary Abbé refractometer. The phase difference curve is not very sensitive to n_0. By the method we have outlined it is possible to measure all three elastic constants in the same specimen. FRÉEDERICKSZ and ZWETKOFF have described an experimental setup with which these measurements could all be made [9].

B. k_{11}, k_{22}, and k_{33} Obtained from the Normal Deformation of a Twisted Parallel Oriented Sample

A new sample configuration can be obtained if one glass plate of a parallel oriented sample is twist-

ed with respect to the other by an angle Θ. The optical axis still remains parallel to the boundaries, but it now turns smoothly and continuously from surface to surface. LESLIE has solved this case for magnetic fields using a procedure based on a balancing of the forces in the sample [25]. Only non-dissipative forces enter into the static problem and the same solution can be obtained by considering only the energies and making a virtual deformation similar to what was done in Section I. Two coupled differential equations result, because now two independent parameters, the polar angle and the azimuthal angle of the local optical axis, enter into the analysis. All three elastic constants play a role and influence the deformation in this case, which was not true in the previous examples studied. LESLIE computes a threshold field H_0 for the deformation given by [25]

$$\Delta\chi (H_0 x_0)^2 = \pi^2 k_{11} + (k_{33} - 2 k_{22})\ \Theta ,$$

which reduces to the threshold expression (12 a) in Case 2 for $\Theta = 0$. SNYDER and SAUPE [11] have verified this expression for PAA obtaining values of k_{22} that are in good agreement with FRÉEDERICKSZ [9].

In principle, measurements of the deformation in this case can give values for all three elastic constants in one specimen for only one orientation in the field. GERRITSMA, DE JEU, and VAN ZANTEN have used the change in electrical capacitance to detect this deformation in a magnetic field [18]. SHTRIKMAN, WOHLFARTH, and WAND [26] give an expression for the capacitance change ΔC for $\Theta = \pi/2$ in the threshold region where the polar deformation angle is small:

$$\frac{\Delta C}{\Delta C_{\max}} = 2 \left\{ \frac{4 (k_{11}/k_{22}) - 2 + (k_{33}/k_{11})}{-1 + 5 (k_{33}/k_{22}) - (k_{33}/k_{22})^2} \right\} \frac{H - H_0}{H_0} + o \left(\frac{H - H_0}{H_0} \right)^2 .$$

This deformation can also be observed optically in a manner similar to Case 2 if the polarizer is oriented so that an ordinary and extraordinary ray are propagated in the material. The polarization plane of both the ordinary and extraordinary ray twists with the structure, but for pitches longer than the wavelength of light this twist does not appreciably affect the phase difference between the rays at the other side of the sample. This case should not be confused with the similar twisted electro-optic device where the polarizer is oriented so that only one ray is propagated inside the material [27].

C. Method of Determining k_{22} by Doping the Nematic with a Chiralic Molecule

DURAND et al. have shown another possible way to measure k_{22} for nematics making use of the unwinding of a cholesteric liquid crystal [28]. They dissolve a small amount of chiralic impurity in the nematic liquid crystal under study, which produces a cholesteric liquid crystal with a helical structure having a pitch P_0. DE GENNES [29] has shown that if a magnetic field is applied perpendicular to the helical axis, a threshold field H_0 exists where the helix completely unwinds producing a cholesteric to nematic transformation. H_0 is given by [29]

$$H_0 = \pi^2 (k_{22}/\Delta\chi)^{1/2} \cdot P_0^{-1} .$$

Of course a measurement of this threshold can give k_{22} only for the particular cholesteric mixture studied. DURAND et al. [28] have found, however, that for dopings of less than 1%, the measured value of k_{22} is independent of the initial pitch length P_0. In this case the k_{22} of the mixture would be the same as for the pure nematic.

Acknowledgement

The authors are grateful to A. SAUPE for fruitful discussions and encouragement during his visits to our institute. We also wish to thank H. DEULING for the least squares fitting program and for sending us a preprint of an electric field calculation.

[1] H. ZOCHER, Trans. Faraday Soc. **29**, 945 [1933]; a historical review is given in this paper.
[2] A. SAUPE, Z. Naturforsch. **15 a**, 815 [1960]; earlier work that assumed $k_{11} = k_{33}$ is mentioned here.
[3] F. J. KAHN, Appl. Phys. Lett. **20**, 199 [1972].
[4] M. F. SCHIEKEL and K. FAHRENSCHON, Appl. Phys. Lett. **19**, 391 [1971].
[5] H. GRULER and G. MEIER, Molec. Cryst. and Liquid Cryst. **16**, 299 [1972].
[6] F. C. FRANK, Disc. Faraday Soc. **25**, 19 [1958].
[7] E. SACKMANN, S. MEIBOOM, and L. C. SNYDER, J. Amer. Chem. Soc. **89**, 5981 [1967].
[8] C. M. DAFERMOS, SIAM J. Appl. Math. **16**, 1305 [1968]; a more rigorous mathematical treatment is given here where all solutions are tested for stability.
[9] V. FRÉEDERICKSZ an V. ZWETKOFF, Phys. Z. Sowjetunion **6**, 490 [1934].

[10] Private communication by H. DEULING, Freie Universität Berlin, D-1000 Berlin 33, Arminallee 3. Copies of the program in Fortran IV are available from him upon request.
[11] W. SNYDER and A. SAUPE, private communication.
[12] P. E. CLADIS, J. RAULT, and J. P. BURGER, Molec. Cryst. and Liquid Cryst. **13**, 1 [1971].
[13] W. HAAS, J. ADAMS, and J. B. FLANNERY, Phys. Rev. Lett. **25**, 1236 [1970].
[14] A. RAPINI and M. PAPOULAR, J. Physique **30**, C 4–54 [1969].
[15] H. DEULING obtained this equation in a similar manner: H. DEULING, to be published in Molec. Cryst. and Liq. Cryst.
[16] M. SCHADT, J. Chem. Phys. **56**, 1494 [1972].
[17] D. DIGUET, F. RONDELEZ, and G. DURAND, C. R. Acad. Sci. **B 271**, 954 [1970].
[18] C. J. GERRITSMA, W. H. DE JEU, and P. VAN ZANTEN, Phys. Lett. **36 A**, 389 [1971].
[19] H. BÜCHER, private communication.
[20] G. FÖEX, Trans. Faraday Soc. **29**, 958 [1933].
[21] H. GASPAROUX and J. PROST, J. Physique **32**, 953 [1971].
[22] W. MAIER and G. MEIER, Z. Naturforsch. **16 a**, 470, 1200 [1961].
[23] V. FRÉEDERICKSZ and V. ZOLINA, Trans. Faraday Soc. **29**, 919 [1933].
[24] V. FRÉEDERICKSZ and V. ZWETKOFF, Acta Physicochim. URSS **3**, 895 [1935]. – V. ZWETKOFF, Acta Physicochim. URSS **6**, 865 [1937].
[25] F. M. LESLIE, Molec. Cryst. and Liq. Cryst. **12**, 57 [1970].
[26] S. SHTRIKMAN, E. P. WOHLFARTH, and Y. WAND, Phys. Lett. **37 A**, 369 [1971].
[27] M. SCHADT and W. HELFRICH, Appl. Phys. Lett. **18**, 127 [1971].
[28] G. DURAND, L. LEGER, F. RONDELEZ, and M. VEYSSIE, Phys. Rev. Lett. **22**, 227 [1969].
[29] P. G. DE GENNES, Solid State Comm. **6**, 163 [1968].

Zur Geschwindigkeit der Ausrichtung nematischer Flüssigkeiten durch Magnetfelder

Eine Methode zur Bestimmung der Rotationsviskosität γ_1

G. HEPPKE und F. SCHNEIDER

Iwan N. Stranski-Institut, II. Institut für Physikalische Chemie der Technischen Universität Berlin

(Z. Naturforsch. **27 a**, 976—982 [1972]; eingegangen am 14. März 1972)

Kinetics of Alignment of a Nematic Liquid Crystal in Magnetic Fields
A Method to Determine the Viscosity Coefficient γ_1

The rotation of the molecules in a nematic liquid crystal is studied after rotating the axis of the aligning magnetic field. The process of realignment is observed by doping the liquid crystal with an electrolyte and measuring the cross voltage U^* which is induced perpendicular to the applied electric field. The resulting cross voltages are compared with the stationary values and it can be shown that the degree of order with respect to the rotating director remains almost constant. Therefore, the time dependence of the angle Φ between director and magnetic field can be calculated from the measured cross voltage using the steady state equation $U^* = U^*(\Phi)$. $\Phi(t)$ satisfies the formula

$$\ln|\tan\Phi| = \ln|\tan\Phi_0| - (\chi_a H^2/\gamma_1)\, t$$

which is derived from the differential equation for the rotation of the director. This formula allows the calculation of the viscosity coefficient γ_1, giving a value of 1.08 P for MBBA at 25 °C. An activation energy of 11.5 kcal mol^{-1} is determined from the temperature dependence of the viscosity coefficient.

1. Einleitung

Bereits von SVEDBERG[1] wurde festgestellt, daß die durch ein Magnetfeld in einer nematischen Flüssigkeit erzielte homogene Ausrichtung nach dem Ausschalten des Magnetfeldes für längere Zeit erhalten bleibt. Wird das Magnetfeld nach einer Drehung des Magneten wieder eingeschaltet, so erfahren die Moleküle infolge der Anisotropie ihrer magnetischen Suszeptibilität ein Drehmoment. Dieses bewirkt eine Drehbewegung der Ausrichtungsachse, d. h. des Direktors auf die neue Magnetfeldrichtung hin. Wie die vorliegende Arbeit zeigt, vollzieht sich diese Drehbewegung unter Erhaltung des Ordnungsgrades bezüglich der momentanen Ausrichtungsachse nahezu homogen. Die Relativbewegung des Direktors zur Flüssigkeit, welche bei diesem Experiment in Ruhe bleibt, wird durch die Rotationsviskosität γ_1 [2–4] gehemmt. Die sich einstellende Winkelgeschwindigkeit erlaubt daher eine Messung dieses Viskositätskoeffizienten.

Die Lage der Ausrichtungsachse wird mit der Querspannungsmethode[5] bestimmt, die sich besonders für große Probenvolumina eignet, welche zur Verringerung des Randeinflusses wünschenswert

Sonderdruckanforderungen an Dr. F. SCHNEIDER, II. Institut für Physikalische Chemie der Technischen Universität Berlin, *D-1000 Berlin 12*, Straße des 17. Juni 112.